2918 *Biochemistry* **2010,** *49,* 2918–2924
DOI: 10.1021/bi902127u

BIOCHEMISTRY
including biophysical chemistry & molecular biology
Article

Effects of Introducing Fibrinogen Aα Character into the Factor XIII Activation Peptide Segment[†]

Madhavi A. Jadhav, Giulia Isetti, Toni A. Trumbo, and Muriel C. Maurer*

Department of Chemistry, University of Louisville, 2320 South Brook Street, Louisville, Kentucky 40292

Received December 11, 2009; Revised Manuscript Received February 22, 2010

ABSTRACT: The formation of a blood clot involves the interplay of thrombin, fibrinogen, and Factor XIII. Thrombin cleaves fibrinopeptides A and B from the N-termini of the fibrinogen Aα and Bβ chains. Fibrin monomers are generated that then polymerize into a noncovalently associated network. By hydrolyzing the Factor XIII activation peptide segment at the R37−G38 peptide bond, thrombin assists in activating the transglutaminase FXIIIa that incorporates cross-links into the fibrin clot. In this work, the kinetic effects of introducing fibrinogen Aα character into the FXIII AP segment were examined. Approximately 25% of fibrinogen Aα is phosphorylated at Ser3, producing a segment with improved binding to thrombin. FXIII AP (^{22}AEDDL^{26}) has sequence properties in common with Fbg Aα (^{1}ADSpGE^{5}). Kinetic benefits to FXIII AP cleavage were explored by extending FXIII AP (28−41) to FXIII AP (22−41) and examining peptides with D24, D24S, D24Sp, and D24Sp P27G. These modifications did not provide the same kinetic advantages that were observed with Fbg Aα (1−20) S3p. Such results further emphasize that FXIII AP derives most of its substrate specificity from the P_9−P_1 segment. To enhance the kinetic properties of FXIII AP (28−41), we introduced substitutions at the P_9, P_4, and P_3 positions. Studies reveal that FXIII AP (28−41) V29F, V34G, V35G exhibits kinetic improvements that are comparable to those of FXIII AP V29F, V34L and approach those of Fbg Aα (7−20). Selective changes to the FXIII AP segment sequence may be used to design FXIII species that can be activated more or less readily.

Thrombin, fibrinogen, and Factor XIII (FXIII)[1] play critical roles in the last stages of the blood coagulation cascade (*1*−*4*). Fibrinogen is a structural protein that circulates in the blood as a dimer of trimers [(AαBβγ)$_2$]. The serine protease thrombin cleaves the R16−G17 peptide bond of the fibrinogen Aα chains and the R14−G15 peptide bond of the fibrinogen Bβ chains, thereby releasing fibrinopeptides A and B. These cleavages lead to exposure of fibrin polymerization sites that promote formation of a noncovalently associated fibrin clot network. Thrombin also supports Factor XIII activation by hydrolyzing the FXIII R37−G38 peptide bond which later aids in exposure of the transglutaminase catalytic site (*3*, *4*). Activated FXIII catalyzes the formation of γ-glutamyl−ε-lysyl covalent cross-links in the fibrin network and in fibrin−enzyme complexes.

Thrombin is a versatile serine protease that targets several players in coagulation, anticoagulation, and platelet activation (*1*, *5*, *6*). This sodium-activated type II enzyme utilizes insertion loops on its surface to limit substrate access to the active site cleft. Moreover, thrombin contains two anion binding exosites (ABE-I and ABE-II) that it employs to promote interactions with selected proteins (Figure 1). For example, regions of fibrinogen Aα, PAR1, hirudin, and thrombomodulin bind to ABE-I, whereas fibrinogen γ′, heparin, GpIbα, and FVIII target ABE-II.

A review of thrombin substrates reveals that amino acids located N-terminal to the scissile bond make important contributions to binding and to rates of hydrolysis (*7*). The P_2, P_4, and P_9 positions[2] have been extensively studied. A common polymorphism exists in FXIII where a Val at the P_4 position is replaced with a Leu (V34L) (*3*). FXIII V34L is found in approximately 25% of the Caucasian population and results in a FXIII that is more easily activated by thrombin. This polymorphism has been correlated with protection against myocardial infarction (*3*, *4*). These effects occur predominantly under high-fibrin(ogen) conditions and are associated with thinner fibrin chains and a more permeable clot structure (*8*).

Our laboratory has utilized kinetic studies and solution NMR methods to probe the roles of individual FXIII AP residues in interacting with thrombin. Trends observed with synthetic peptide models of the FXIII V34 and FXIII V34L activation segment are in agreement with results obtained with their intact FXIII species (*9*−*13*). A series of peptides with substitutions at the P_4 position (V, L, F, A, and I) have been screened for reactivity (*14*, *15*). The cardioprotective L34 continues to provide the strongest k_{cat}/K_m due to enhancements in K_m and even stronger influences on k_{cat}. Two-dimensional (2D) trNOESY studies have

[†]Funding for this project was provided by National Institutes of Health Grant R01 HL68440.

*To whom correspondence should be addressed. Telephone: (502) 852-7008. Fax: (502) 852-8149. E-mail: muriel.maurer@louisville.edu.

[1]Abbreviations: FXIII, blood clotting Factor XIII; AP, activation peptide; Fbg Aα, fibrinogen Aα chain; PAR1, protease-activated receptor 1; PAR4, protease-activated receptor 4; RP-HPLC, reversed phase high-performance liquid chromatography; MALDI-TOF, matrix-assisted laser desorption ionization time-of-flight; K_m, Michaelis−Menten kinetic constant; k_{cat}, catalytic constant or turnover number; NMR, nuclear magnetic resonance; NOESY, nuclear Overhauser effect spectroscopy; PDB, Protein Data Bank; trNOESY, transferred NOESY.

[2]The P nomenclature system (...P_3, P_2, P_1, P_1', P_2', P_3', ...) is used to assign the individual amino acid positions on the substrate peptides. The P_1−P_1' peptide bond becomes hydrolyzed by the enzyme. The peptide amino acids N-terminal to the cleavage site are labeled P_2, P_3, P_4, etc., whereas those that are C-terminal are labeled P_2', P_3', P_4', etc.

 Published on Web 03/10/2010

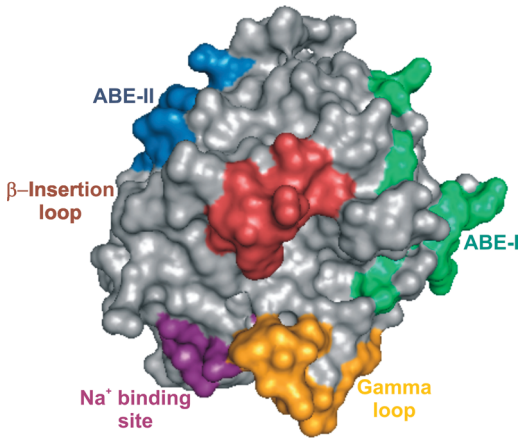

FIGURE 1: Structure of thrombin showing key surface loops and exosites. A contour representation of thrombin (PDB entry 1PPB) is displayed with the active site region in the center. β and γ loops that regulate substrate specificity and access to the catalytic site are colored maroon and yellow, respectively. Anion binding exosite I is located to the right of the active site region and is colored green, whereas anion binding exosite II is located to the left and is colored blue. The allosteric sodium binding site is colored purple. The molecular graphics program PyMOL was used to create the structures displayed in Figures 1−3.

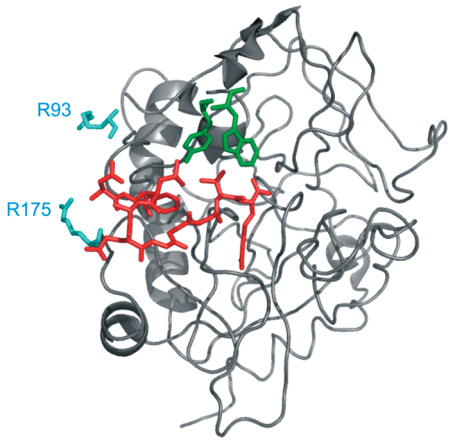

FIGURE 2: Evaluating thrombin interaction sites for the N-terminal Fbg Aα sequence. The X-ray crystal structure of human Fbg Aα (7−16) (red) bound to bovine thrombin (gray) is displayed (PDB entry 1BBR). The thrombin β-insertion loop residues Trp60d and Tyr60a are colored green. Two residues of anion binding exosite II (R93 and R175) that could accommodate Fbg Aα S3p are colored light blue.

revealed an important P_4-P_2 interaction (L34/F34−P36) that is proposed to promote interactions with the thrombin active site region (*11*, *15*).

In addition to the active site region, the anion binding exosites are also valuable to consider. A fibrinogen Aα region located C-terminal to the thrombin-cleaved scissile bond targets ABE-I (*2*, *5*). By contrast, phosphorylation near the N-terminus allows this fibrinogen chain to be accommodated by thrombin ABE-II (*16*). The fibrinogen Aα chain can be phosphorylated at two sites: the N-terminal S3 (*17*) and the more distant S345 (*18*). Increased levels of phosphorylation have been observed under certain physiological and pathophysiological conditions (*19*, *20*). Human fetal fibrinogen contains twice the degree of Aα phosphorylation of adult fibrinogen (*21*). The amount of phosphorylated fibrinogen has been reported to double following hip replacement surgery (*18*). Elevated levels of phosphorylated fibrinogen have also been observed in cancer patients and in individuals recovering from acute myocardial infarction (*22*−*25*).

Approximately 25−30% of plasma-derived human fibrinogen Aα (Fbg Aα) is phosphorylated at the Ser3 position (*26*, *27*). Similar levels have been found in human fibrinogen chains expressed in CHO cells, suggesting that partial phosphorylation is a native phenomenon (*28*). Kinetic studies of intact Fbg Aα and on Fbg Aα-like peptides [Aα (1−20)] have revealed that phosphorylation at the S3 position lowers the K_m of thrombin hydrolysis (*16*, *29*). Moreover, one-dimensional (1D) and 2D NMR studies have shown that Ser3p helps to anchor Aα (1−5) to the thrombin surface (*16*, *30*). A review of the Fbg Aα residues $^{1}ADS_pGE^{5}$ reveals that they have properties in common with FXIII AP ($^{22}AEDDL^{26}$). They both start with an alanine and then contain a series of negatively charged residues that could be accommodated by positively charged residues on an enzyme. These characteristics lead to an interest in exploring whether binding interactions between FXIII AP and the thrombin surface could be further enhanced via introduction of a site of phosphorylation in which D24 is replaced with a phosphorylated serine (D24Sp). It is already known that residues within the FXIII P_9-P_1 segment make important contributions to binding and hydrolysis. The possibility of obtaining additional benefits from targeting ABE-II warrants further investigation.

Another strategy for enhancing the binding and hydrolysis of FXIII AP would be to introduce more Fbg Aα-like character into the P_9-P_1 region. The Phe8 residue at the P_9 position of Fbg Aα is vital for generating its effective thrombin substrate properties (*31*, *32*). A characteristic helical turn structure (*33*) is adopted in which F8 is directed toward the P_4-P_1 region ($^{13}GGVR^{16}$) (Figure 2). V29F can be introduced into the FXIII AP sequence, but there is concern with regard to how well the aromatic residue can be accommodated by the $^{34}VVPR^{37}$ FXIII stretch (*11*). To alleviate possible steric issues, a FXIII AP peptide was proposed containing V29F, V34G, and V35G mutations. The Pro at the P_2 position would remain since this residue plays a key anchoring role in the FXIII activation peptide sequence. The new sequence would thus contain substitutions at the P_9, P_4, and P_3 positions.

This work supports the proposal that FXIII derives most of its substrate specificity from P_9-P_1 with a focus on the P_4-P_1 segment. FXIII activation peptides that are extended to the P_{16} position and further designed to target ABE-II do not exhibit the kinetic benefits observed for comparable fibrinogen Aα-like sequences. Introducing other characteristic features of the Aα chain into the FXIII AP segment is a more promising strategy for altering the activation properties of Factor XIII. For the mutant sequence FXIII AP (28−41) V29F, replacements of V34 and V35 with glycines promoted more effective binding and hydrolysis within the thrombin active site. Interestingly, the kinetic properties are comparable to those of FXIII AP (28−41) V29F, V34L. From these different studies, valuable information about the substrate specificity of thrombin for FXIII AP is being revealed.

EXPERIMENTAL PROCEDURES

Synthetic Peptides. Peptides based on residues 22−41 of the human FXIII activation peptide were synthesized by New England Peptide (Gardner, MA) or by Giulia Isetti (University of Louisville). The peptide based on residues 28−41 was synthesized by SynPep (Dublin, CA). The peptide sequences are as follows: FXIII AP (22−41), Ac-AEDDLPTVELQGVVPRGVNL-amide; FXIII AP (22−41) D24S, Ac-AESDLPTVELQGVVP-RGVNL-amide; FXIII AP (22−41) D24Sp, Ac-AESpDLPT-

VELQGVVPRGVNL-amide; FXIII AP (22−41) D24Sp P27G, Ac-AESpDLGTVELQGVVPRGVNL-amide; FXIII AP (28−41) V29F, V34G, V35G, Ac-TFELQGGGPRGVNL-amide. The purity of the peptides was evaluated by analytical reversed phase HPLC. MALDI-TOF mass spectrometry measurements on an Applied Biosystems Voyager DE-Pro mass spectrometer were used to verify the peptide m/z values. The concentrations of the peptide stock solutions were determined by quantitative amino acid analysis (AAA Service Laboratory, Damascus, OR, and University of Iowa, Molecular Analysis Facility, Iowa City, IA). All peptides were soluble to 8 mM.

Thrombin Preparation. Plasma bovine citrate or sulfate eluate (Sigma) was dissolved in 50 mM Tris, 150 mM NaCl, and 0.1% PEG (pH 7.4) and desalted on a GE Healthcare Biotech PD-10 column into the same buffer. The prothrombin-containing solution was then activated at 37 °C by *Echis carinatus* snake venom in the presence of $CaCl_2$. The ability to clot fibrinogen was monitored over time. A Sephadex G-25 column equilibrated with 25 mM H_3PO_4 and 100 mM NaCl (pH 6.5) was employed to desalt the venom-activated mixture. The generated thrombin was then purified on an Amersham Pharmacia Biotech Mono S cation exchange column (HR10/10) using a linear gradient from 0 to 1 M NaCl in 25 mM H_3PO_4 (pH 6.5). The pooled thrombin solution was concentrated by ultrafiltration, aliquoted, and stored at −70 °C. The final concentration of thrombin was determined using an extinction coefficient $E^{1\%}$ of 19.5 at 280 nm.

The bovine form of thrombin was used for this project, and the synthetic substrates were based on human sequences. There is a high degree of sequence conservation between bovine and human thrombin (*34*). No differences appear in the residues involving the active site, the thrombin β-insertion loop (also called the Trp^{60D} loop), or the allosteric Na^+ binding site. Any changes within ABE-II involve complementary substitutions between Lys and Arg residues. The other minor differences that do exist between the species are not anticipated to interfere with the interaction of the substrate peptides at the thrombin active site surface. Further supporting this notion, NMR studies (*35*−*37*) involving bovine thrombin and peptides targeting the active site (fibrinopeptide A and PAR1) have been in agreement with X-ray studies of the same peptides in the presence of human thrombin (*38*, *39*). Furthermore, NMR studies involving γ' peptides that target ABE-II have revealed similar results for both bovine α-IIa and human γ-IIa (*40*).

Kinetics Procedure. The HPLC-based kinetic assay methods described by Trumbo and Maurer (*9*) were employed. Briefly, a solution of peptide and assay buffer [50 mM H_3PO_4, 100 mM NaCl, and 0.1% PEG (pH 7.4)] was heated to 25 °C in a heat block. The peptide concentrations were within the range of 50−1500 μM for the FXIII AP (22−41) peptide series [D24, D24S, D24Sp, and D24Sp P27G]. For FXIII AP (28−41) V29F, V34G, V35G, the concentrations included 45−455 μM. Hydrolysis was started by the addition of bovine thrombin. The thrombin concentration for the hydrolysis reactions was 33.6 nM for the FXIII AP (22−41) peptide series and 2.2 nM for FXIII AP (28−41) V29F, V34G, V35G. At regular intervals, an aliquot of the reaction mixture was removed and quenched in 12.5% H_3PO_4. A Brownlee Aquapore Octyl RP-300 C_8 Cartridge column was used to separate the peptide peaks on a Waters HPLC system. The thrombin concentration and kinetic time points were chosen so that less than 15% of the total peptide concentration was hydrolyzed within 30 min. The FXIII AP (28−37) product peak was integrated and the peak area converted to concentration using a calibration curve.

The slopes of product concentration versus time plots were used to determine the initial velocities (in micromolar per second) for the different thrombin-catalyzed reactions. The results reported represent averages for at least three independent experiments. Kinetic values were calculated using nonlinear regression analysis fit to the equation $V = V_{max}/(1 + K_m/[S])$ using the Marquardt−Levenberg algorithm in Sigma Plot (Jandel Scientific). K_m, V_{max}, and k_{cat} were calculated from the coefficients of this equation. ANOVA calculations followed by Tukey−Kramer multiple comparisons were utilized for statistical analysis of the kinetics data (GraphPad, InStat Biostatistics, version 3.0). The different kinetic constants determined for the current project were examined relative to values obtained from previous published studies that had all been conducted with bovine thrombin.

RESULTS

Thrombin-Catalyzed Hydrolysis of FXIII Activation Peptides. An HPLC assay was used to monitor the hydrolysis rates of peptides based on FXIII AP (22−41) and peptide FXIII AP (28−41) V29F, V34G, V35G. For each peptide, thrombin cleaved at the R37−G38 amide bond and the substrates and hydrolyzed products eluted as distinct peaks on the Brownlee Aquapore C_8 column. Hydrolyzed segments corresponding to FXIII AP (22−37) and FXIII AP (28−37) were verified by MALDI-TOF mass spectrometry. Accumulation of these individual products over time was used in the kinetic fit calculations.

Kinetic Analysis of FXIII AP Peptides That Could Extend from the Thrombin Active Site toward Anion Binding Exosite II. Earlier studies in our laboratory reported the kinetic parameters associated with thrombin hydrolysis of FXIII AP (28−41) (*9*). In the study presented here, the FXIII AP segment length was increased N-terminally to FXIII AP (22−41). Table 1 displays this sequence along with others related to this project. Nonlinear regression analysis values for K_m, k_{cat}, and k_{cat}/K_m are listed in Table 2. The seven additional N-terminal residues present in FXIII AP (22−41) contributed to a 1.7-fold decrease in K_m relative to FXIII AP (28−41) ($P < 0.001$). This decrease corresponded to a moderate improvement in binding interactions.

A phosphorylated S3 at the P_{14} position of Fbg Aα (1−20) is known to promote binding of this peptide substrate to thrombin (*16*, *29*). FXIII AP (22−41) contains a D24 at the same position as S3 of Fbg Aα (1−20). A FXIII AP (22−41) D24S substitution was well-tolerated, and the kinetic binding properties remained statistically different from those of FXIII AP (28−41) ($P < 0.01$). Introducing a site of phosphorylation at S24 (D24Sp) resulted in some minor increases in K_m. Upon reviewing the FXIII AP (22−41) D24Sp sequence, we were concerned that the P27 residue might promote a turn structure that hinders optimal interactions with thrombin ABE-II. To alleviate this possibility and introduce more flexibility, a glycine was introduced to produce FXIII AP (22−41) D24Sp P27G. Only a very minor improvement in K_m occurred relative to FXIII AP (22−41) D24Sp. A review of the kinetic data revealed that there were no statistical differences in K_m values among the different variants of FXIII AP (22−41).

The k_{cat} values also provided valuable information about interactions between the FXIII AP segments and thrombin. The N-terminal extension to FXIII AP (28−41) to generate FXIII AP (22−41) resulted in a minor 1.3-fold decrease in k_{cat}

Table 1: Substrate Sequences Capable of Extending to Thrombin ABE-II[a]

	P_9.....P_4.....P_1...
Factor XIII AP (22-41)	^{22}AED DLPTVELQGVVPRGVNL^{41}
Factor XIII AP (22-41) D24S	^{22}AES DLPTVELQGVVPRGVNL^{41}
Factor XIII AP (22-41) D24S$_p$	^{22}AES$_p$DLPTVELQGVVPRGVNL^{41}
Factor XIII AP (22-41) D24S$_p$ P27G	^{22}AES$_p$DLGTVELQGVVPRGVNL^{41}
Fibrinogen Aα (1-20) S3$_p$	^{1}ADS$_p$GEGDFLAEGGGVRGPRV^{20}

[a]Human sequences of factor XIII and fibrinogen Aα are displayed. Sp corresponds to a phosphorylated serine.

Table 2: Kinetic Constants for Hydrolysis of FXIII AP Substrates Capable of Extending to Thrombin ABE-II[a]

peptide sequence	K_m (μM)	k_{cat} (s^{-1})	k_{cat}/K_m (s^{-1} μM^{-1})
FXIII AP (28−41)[b]	508 ± 44	6.4 ± 0.03	0.013 ± 0.001
FXIII AP (22−41)	300 ± 54	4.9 ± 0.01	0.016 ± 0.003
FXIII AP (22−41) D24S	270 ± 43	4.7 ± 0.31	0.017 ± 0.003
FXIII AP (22−41) D24Sp	422 ± 65	6.9 ± 0.48	0.016 ± 0.003
FXIII AP (22−41) D24Sp P27G	370 ± 34	3.5 ± 0.15	0.009 ± 0.001

[a]Kinetic constants for the thrombin-catalyzed hydrolysis reactions were determined from an HPLC assay as described in Experimental Procedures. The results shown here represent averages of at least three independent experiments. Kinetic values were calculated using nonlinear regression analysis methods using SigmaPlot. The error values correspond to the standard error of the mean (SEM). [b]From ref *9*.

($P > 0.05$). This value was maintained with the D24S substitution. The k_{cat} value for FXIII AP (22−41) D24Sp increased to that of FXIII AP (28−41). The additional P27G mutation generated a FXIII AP (22−41) D24Sp P27G peptide that exhibited an ~2-fold decrease in the k_{cat} value relative to that of FXIII AP (28−41). A convincing case for statistical differences in the k_{cat} values of the FXIII AP (28−41) and (22−41) peptide series could not be found.

Introducing Fibrinogen Aα-like Character into FXIII AP (28−41). Prior studies evaluated the effects of introducing V29F into FXIII AP (28−41), thus placing an aromatic residue (*11*) at the same position as the vital F8 of Fbg Aα (7−20) (Tables 3 and 4). The K_m value for hydrolysis of FXIII AP (28−41) V29F improved 2.6-fold relative to that of wild-type FXIII AP (28−41) ($P < 0.01$), whereas the k_{cat} value remained virtually unchanged. In the study presented here, additional features of the Fbg Aα chain were introduced. The newly modified FXIII AP segment contained the Phe residue (V29F), and the aliphatic branched V34 and V35 residues were replaced with smaller G34 and G35 residues, respectively [FXIII AP V29F, V34G, V35G (T*F*ELQG*GG*PRGVNL, mutated residues in italics)]. The K_m of FXIII AP V29F, V34G, V35G (326 ± 79 μM) was between that of FXIII AP (28−41) (508 ± 44 μM) and that of FXIII AP (28−41) V29F (195 ± 34 μM) ($P < 0.01$ for both comparisons). By contrast, the k_{cat} value of FXIII AP (22−41) V29F, V34G, V35G increased 4.5-fold relative to those of FXIII AP (28−41) and FXIII AP (28−41) V29F ($P < 0.001$). An evaluation of the resultant k_{cat}/K_m values revealed that the substrate specificity toward FXIII AP (28−41) V29F, V34G, V35G was significantly different ($P < 0.001$) from that of FXIII activation peptides containing a V34G, V29F, or V34L substitution (Table 4). Interestingly, the K_m value of FXIII AP (28−41) V29F, V34G, V35G was now comparable to that of Fbg Aα (7−20). Furthermore, the k_{cat} had improved such that it was now only 1.4-fold lower than that of Fbg Aα (7−20).

Table 3: Introducing Fibrinogen Aα-like Character into the Factor XIII Activation Peptide[a]

	P_9.....P_4....P_1...
Factor XIII AP (28-41)	^{28}TVELQGVVPRGVNL^{41}
Factor XIII AP (28-41) V34L	^{28}TVELQGLVPRGVNL^{41}
Factor XIII AP (28-41) V29F	^{28}TFELQGVVPRGVNL^{41}
Factor XIII AP (28-41) V29F V34L	^{28}TFELQGLVPRGVNL^{41}
Factor XIII AP (28-41) V29F, V34G, V35G	^{28}TFELQGGGPRGVNL^{41}
Fibrinogen Aα (7-20)	^{7}DFLAEGGGVRGPRV^{20}

[a]Human sequences for factor XIII and fibrinogen Aα are displayed.

Table 4: Kinetic Constants for Hydrolysis of FXIII AP Substrates Having Fibrinogen Aα-like Character[a]

peptide sequence	K_m (μM)	k_{cat} (s^{-1})	k_{cat}/K_m (s^{-1} μM^{-1})
FXIII AP (28−41)[b]	508 ± 44	6.4 ± 0.03	0.013 ± 0.001
FXIII AP (28−41) V34L[b]	272 ± 57	18.5 ± 1.6	0.068 ± 0.02
FXIII AP (28−41) V29F[c]	195 ± 34	6.2 ± 0.4	0.032 ± 0.006
FXIII AP (28−41) V29F, V34L[c]	352 ± 77	27.5 ± 2.9	0.078 ± 0.02
FXIII AP (28−41) V29F, V34G, V35G	326 ± 79	28.6 ± 3.7	0.088 ± 0.02
Fbg Aα (7−20)[b]	312 ± 42	39.3 ± 2.6	0.126 ± 0.02

[a]Kinetic constants for the thrombin-catalyzed hydrolysis reactions were determined from an HPLC assay as described in Experimental Procedures. The results shown here represent averages of at least three independent experiments. Kinetic values were calculated using nonlinear regression analysis methods using SigmaPlot. The error values correspond to the standard error of the mean (SEM). [b]From ref *9*. [c]From ref *11*.

DISCUSSION

Factor XIII is activated in part when the serine protease thrombin cleaves the FXIII R37−G38 peptide bond (*2*−*4*). This work provides an opportunity to evaluate the extent to which additional features from Fbg Aα, a major physiological substrate, can be introduced into the FXIII AP sequence to promote binding interactions (K_m) and/or catalytic turnover (k_{cat}). The knowledge gained may be used in the design of new FXIII AP segments that can be activated to different extents.

Evaluating Whether FXIII AP Segments That Take Advantage of Binding to Anion Binding Exosite II Can Be Generated. A review of the FXIII AP sequence reveals that the N-terminal segment (^{22}AEDDL^{26}) has negative charge character resembling that of the N-terminal Fbg Aα segment (^{1}ADSGE^{5}). The N-terminal Fbg Aα (1−5) segment is quite flexible and designed to permit multiple conformations depending on the environment encountered. NMR and docking studies suggest that introducing a phosphoserine at position 3 (S3p) encourages contact with the thrombin surface. The phosphate is proposed to bind in the vicinity of R175 and R93 (*16*) (Figures 1 and 2). In response to the new substrate anchor point, a valuable improvement in the K_m value occurs (*16*).

For this study, the features of Fbg Aα S3p were systematically introduced into the FXIII AP D24 position. Prior work had focused on FXIII AP (28−37) and on the truncated FXIII AP

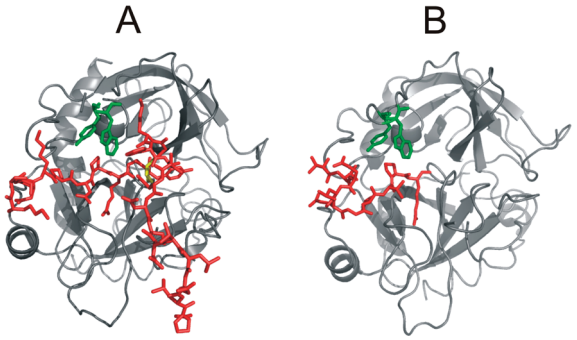

FIGURE 3: Comparison of the conformational features of two thrombin−substrate complexes. (A) Cartoon representation of murine PAR4 (51−81) (red) bound to murine thrombin (gray) (PDB entry 2PV9). Pro62 which is hypothesized to play a role in redirecting the PAR4 segment from the active site toward the thrombin autolysis loop is colored yellow. Thrombin β-insertion loop residues Trp60d and Tyr60a are colored green. (B) Cartoon representation of the X-ray crystal structure of FXIII AP (28−37) (red) bound to thrombin (gray) (PDB entry 1DE7). Thrombin β-insertion loop residues Trp60d and Tyr60a are colored green. So far, the helical-turn conformation captured in the crystal structure has not been observed in solution by NMR methods.

(33−37) sequence (*9*, *41*). Extending the FXIII AP segment toward A22 at the P_{16} position did provide some benefits to K_m, but the k_{cat} was negatively affected. A D24S substitution was well-tolerated, indicating that an acidic aspartate residue was not required for the P_{14} position of FXIII AP. Introducing the phosphorylated Ser (D24Sp) generated modest improvements in k_{cat}, but the K_m also increased. Overall, the slight improvements in k_{cat}/K_m obtained with the N-terminal extension and the site of phosphorylation were not statistically significant (Table 2).

A recent X-ray crystal structure of a murine PAR4 segment (^{51}K−A^{81}) bound to murine thrombin (Figure 3A) revealed an important conformational feature to consider (*42*). G60 located at the P_1' position of this substrate sequence helps to initiate a turn followed by a short helical segment. Instead of extending from the thrombin active site to ABE-I, the PAR4 segment is redirected toward the thrombin autolysis loop located below the entrance to the active site. P62 plays a critical role in helping to achieve this structural change (see the residue colored yellow in Figure 3A). Interestingly, the FXIII AP segment contains a stretch with a Pro residue at the P_{11} position (^{22}AEDDLPTVEL^{31}). This ring structure may hinder the ability of the phosphorylated FXIII AP segment to target a complementary Arg or Lys residue within thrombin ABE-II (*16*). Extra flexibility was introduced through the D24Sp P27G double mutant, but the new sequence did not provide extensive benefits. If anything, an ability to orient effectively within the thrombin active site region had become hindered.

The results obtained with this sequence design project lead to a reanalysis of the properties of FXIII and fibrinogen Aα. When bound to thrombin, the fibrinogen Aα segment (^{1}ADSGEGDFLAEGGGVR^{16}) adopts a unique helical-turn structure (*33*) with key participation from F8, L9, and ^{13}GGVR^{16} (Figure 2). Such a structure has not been observed in solution NMR studies of FXIII AP V34, V34L, or V34F bound to thrombin (*11*, *15*). Fbg Aα clearly requires an extension out to at least the P_9 residue and can gain further benefits by proceeding to the P_{16} position and utilizing S3p at the P_{14} position. By contrast, kinetic studies with FXIII AP (22−41), FXIII AP (28−41), and the truncated segment FXIII AP (33−41) indicate that thrombin takes advantage of the P_9−P_1 residues with a focus on the P_4−P_1 region (*41*). Furthermore, results suggest that FXIII residues surrounding the P_4 position are more important for controlling thrombin binding and hydrolysis than extending to a segment that could target ABE-II.

Evaluating the Effects of the Introduction of Further Fbg Aα-like Character into FXIII AP (*28*−*41*). The roles of the P_9−P_1 positions in promoting thrombin-catalyzed hydrolysis of FXIII AP segments are worth further exploring. The common V34L polymorphism results in a 2-fold improvement in K_m and more importantly a 3-fold improvement in k_{cat} relative to those of FXIII AP V34 (*9*) (Table 4). Overall, a 5-fold improvement in k_{cat}/K_m occurs with the addition of a methylene group to V34 at the P_4 position. Introduction of V29F at the P_9 position (*11*) leads to a 2.6-fold improvement in K_m relative to that of FXIII AP (28−41) V34; however, there is no change to k_{cat}. Although the V29F substitution makes the FXIII AP segment more Fbg Aα-like, the kinetic benefits found in the Aα chain have not been achieved. Moreover, the characteristic helical-turn structure of Fbg Aα (7−16) is not observed in solution NMR studies of FXIII AP (28−37) V29F bound to thrombin (*15*).

To help promote the optimal orientation of the FXIII V29F AP segment at the thrombin active site, the V34 and V35 residues at the P_4 and P_3 positions, respectively, were replaced with glycines. Some decreases in the level of binding interaction were observed, but more impressively, there was a 4.5-fold enhancement in catalytic turnover. To further improve k_{cat}, the next residue to mutate might be the P_2 position. Difficulties, however, will likely arise since FXIII AP (28−41) P36V exhibits solubility issues.

Unexpectedly, the kinetic properties of the FXIII AP (28−41) V29F, V34G, V35G peptide (^{28}TFELQGGGPRGVNL^{41}) are very similar to those of FXIII AP (28−41) V29F, V34L (^{28}TFELQGLVPRGVNL^{41}) (*11*). For each sequence, the P_9 and P_4−P_1 residues are underlined. Both peptides have comparable K_m values, and they both exhibit the 4.5-fold improvement in k_{cat} over that of FXIII AP (28−41) V34. In an earlier publication, the V34L substitution at the P_4 position was proposed to play a more critical role than the V29F substitution at the P_9 position (*11*). The V34L substitution could influence K_m and k_{cat}, whereas the V29F substitution could influence only K_m. Solution NMR studies indicated that the hallmark P_4−P_2 interaction involving L34 and P36 was preserved in FXIII AP V29F, V34L and a helical turn involving F29 was still not visible (*11*). These studies suggest that V34G and V35G substitutions at the P_4 and P_3 positions, respectively, can mimic the kinetic benefits of the V34L substitution at the P_4 position. The P_3 position exhibits much sequence variability and might not be expected to make a major contribution to substrate specificity. Work by Lee et al. (*43*) revealed that recombinant FXIII A_2 V35L (at P_3) does not exhibit the kinetic benefits of the V34L substitution. By contrast, Andersen and co-workers (*44*) reported that recombinant FXIII A_2 V34L, V35T results in a 7.6-fold increase in activation rate relative to that of FXIII A_2 V34 and a 5-fold increase relative to that of FXIII A_2 V34L. Our research indicates another P_4−P_3 double substitution (V34G, V35G) that can exhibit beneficial effects toward thrombin-catalyzed hydrolysis of the FXIII AP segment. The improvements with FXIII AP V29F, V34G, V35G are comparable to those with FXIII AP V29F, V34L.

Determining the structural features of thrombin-bound FXIII AP (28−37) V29F, V34G, V35G and comparing them to the previously published FXIII AP sequences would be valuable.

Unfortunately, it has not been possible to examine the triply substituted peptide using 1D proton line broadening and 2D trNOESY. The peptide does not exhibit sufficiently fast exchange on and off the enzyme surface. This slow exchange does, however, support the proposal that the substitutions at the P_9, P_4, and P_3 positions have generated a peptide that exhibits increased affinity for the thrombin surface.

The ability to create a FXIII AP (28−41) segment that mimics the properties of Fbg Aα (7−20) leads to the question of whether a true hybrid FXIII AP−Fbg Aα sequence could be effective. Andersen and co-workers recently published their results on such a system (*44*). Fbg Aα (7−15) and Aα (7−20) were incorporated into recombinant FXIII A_2 in place of the FXIII AP (28−37) or FXIII AP (28−41) segment. Interestingly, these variants had thrombin activation rates that were 5% of that of wild-type FXIII A_2. Furthermore, they exhibited greatly reduced clot lysis times.

To be an effective thrombin substrate, the Fbg Aα (7−20) segment must be able to adopt a turn conformation bringing F8 into the proximity of the R16−G17 cleavage site. This structural feature has been documented by both X-ray (*33*) and solution NMR methods (*35*, *36*). So far, a helical-turn conformation has not been observed in solution (*11*, *15*) with FXIII AP (28−37) V34, V34L, V34F, V29F, or the doubly substituted V29F, V34L form. If such a conformation does exist, it must be fleeting in nature. An X-ray crystal structure of a thrombin−FXIII AP (28−37) V34 complex has captured this structural feature (*45*) (Figure 3B). This backbone conformation occurs even though the degree of sequence identity of the P_{10}−P_1 residues of Fbg Aα (7−16) and FXIII AP (28−37) is only 20% (*46*). By contrast, FXIII AP (28−37) V34L appears to adopt a more extended conformation within the crystal complex (*45*). Molecular docking studies (*46*) have further supported this type of structural feature for a V34L substitution-containing activation peptide.

The FXIII AP segment is 37 residues in length, and X-ray crystallography of the intact protein suggests that each activation peptide straddles the FXIII dimer interface (*47*). With the hybrid FXIII AP−Fbg Aα sequence, it is highly likely that a helical turn must form for this segment to become an effective thrombin substrate. The low observed FXIII A_2 activation rates suggest there may be difficulties in achieving this conformational feature. The length of the FXIII AP segment may also be considered. The Fbg Aα segment contains only six residues N-terminal to the Fbg Aα (7−20) segment. The Fbg Aα (1−5) stretch is proposed to be highly flexible but can be anchored to thrombin ABE-II through phosphorylation at S3p (*16*). The FXIII AP (1−27) segment is so much longer. It is not known how well a helical turn could be maintained with residues 28−37 and the extent to which the conformation and placement of residues 1−27 would be affected.

Results with the hybrid FXIII AP−Fbg Aα demonstrate that the complete P_9−P_1 segment of Fbg Aα cannot be introduced successfully into intact FXIII A_2 (*44*). A strategy in which only a few residues are changed may be more effective in generating a FXIII with improved activation rates. In this work, an effort has been made to keep P36 as a P_2 anchor point and then to make selective changes to the P_9, P_4, or P_4/P_3 position. The peptides generated do not appear to have a requirement for a helical-turn structure, yet they can achieve kinetic parameters that approach those of Fbg Aα (7−20). These sequences have the potential for being more successful candidates within FXIII A_2.

Conclusions. Kinetic studies of the roles of individual substrate positions are highly worthwhile for understanding the sources of thrombin specificity. Introducing a site of phosphorylation at the P_{14} position of the thrombin substrate FXIII AP does not provide the benefits that are seen with a complementary Fbg Aα sequence. Extra anchoring of FXIII toward the ABE-II region may not be needed. Moreover, additional competing interactions with thrombin ABE-II may not be physiologically attractive. For promoting initial fibrin formation, it may be more desirable to use the exosite to enhance fibrinopeptide A cleavage.

This study also further supports the proposal that FXIII AP derives most of its substrate specificity from P_9−P_1 with a strong focus on the P_4−P_1 segment. The influential role of the P_4 position is well-documented. The FXIII AP segment can be further optimized via addition of other Fbg Aα-like features. A V29F substitution introduces an aromatic residue that can promote binding interactions with the extended thrombin active site surface. Additional improvements can come with FXIII AP V29F, V34G, V35G. The fact that a V29F and V34L substitution can also mimic such effects reinforces the critical role that the common L34 polymorphism plays in promoting the kinetic properties of the FXIII AP segment. So far, the vital helical-turn conformation of Fbg Aα (7−16) has not been observed in solution for FXIII AP segments bound to thrombin. Selective changes to the FXIII AP sequence that are not reliant on this distinct structural feature may provide greater versatility in the design of new FXIII species. This research has focused on amino acid substitutions to enhance K_m and/or k_{cat}, whereas other residue changes would be needed to generate a FXIII that is more difficult to activate. The final architecture of a fibrin clot will be influenced by thrombin's interplay with components of fibrinogen $(A\alpha B\beta\gamma)_2$ and the FXIII AP segment.

ACKNOWLEDGMENT

We appreciate helpful research discussions and critical evaluation of the manuscript from T. M. Sabo, R. Woofter, and P. Doiphode. We also thank R. Woofter for assistance in the statistical analysis of the data.

REFERENCES

1. Di Cera, E. (2007) Thrombin as procoagulant and anticoagulant. *J. Thromb. Haemostasis 5* (Suppl. 1), 196–202.
2. Weisel, J. W. (2005) Fibrinogen and fibrin. *Adv. Protein Chem. 70*, 247–299.
3. Ariens, R. A., Lai, T. S., Weisel, J. W., Greenberg, C. S., and Grant, P. J. (2002) Role of factor XIII in fibrin clot formation and effects of genetic polymorphisms. *Blood 100*, 743–754.
4. Muszbek, L., Bagoly, Z., Bereczky, Z., and Katona, E. (2008) The involvement of blood coagulation factor XIII in fibrinolysis and thrombosis. *Cardiovasc. Hematol. Agents 6*, 190–205.
5. Lane, D. A., Philippou, H., and Huntington, J. A. (2005) Directing thrombin. *Blood 106*, 2605–2612.
6. Di Cera, E. (2008) Thrombin. *Mol. Aspects Med. 29*, 203–254.
7. Backes, B. J., Harris, J. L., Leonetti, F., Craik, C. S., and Ellman, J. A. (2000) Synthesis of positional-scanning libraries of fluorogenic peptide substrates to define the extended substrate specificity of plasmin and thrombin. *Nat. Biotechnol. 18*, 187–193.
8. Lim, B. C., Ariens, R. A., Carter, A. M., Weisel, J. W., and Grant, P. J. (2003) Genetic regulation of fibrin structure and function: complex gene-environment interactions may modulate vascular risk. *Lancet 361*, 1424–1431.
9. Trumbo, T. A., and Maurer, M. C. (2000) Examining thrombin hydrolysis of the factor XIII activation peptide segment leads to a proposal for explaining the cardioprotective effects observed with the factor XIII V34L mutation. *J. Biol. Chem. 275*, 20627–20631.
10. Ariens, R. A., Philippou, H., Nagaswami, C., Weisel, J. W., Lane, D. A., and Grant, P. J. (2000) The factor XIII V34L polymorphism accelerates thrombin activation of factor XIII and affects cross-linked fibrin structure. *Blood 96*, 988–995.
11. Trumbo, T. A., and Maurer, M. C. (2002) Thrombin hydrolysis of V29F and V34L mutants of factor XIII (28−41) reveals roles of the P(9)

and P(4) positions in factor XIII activation. *Biochemistry 41*, 2859–2868.
12. Balogh, I., Szoke, G., Karpati, L., Wartiovaara, U., Katona, E., Komaromi, I., Haramura, G., Pfliegler, G., Mikkola, H., and Muszbek, L. (2000) Val34Leu polymorphism of plasma factor XIII: Biochemistry and epidemiology in familial thrombophilia. *Blood 96*, 2479–2486.
13. Wartiovaara, U., Mikkola, H., Szoke, G., Haramura, G., Karpati, L., Balogh, I., Lassila, R., Muszbek, L., and Palotie, A. (2000) Effect of Val34Leu polymorphism on the activation of the coagulation factor XIII-A. *Thromb. Haemostasis 84*, 595–600.
14. Trumbo, T. A., and Maurer, M. C. (2003) V34I and V34A substitutions within the factor XIII activation peptide segment (28−41) affect interactions with the thrombin active site. *Thromb. Haemostasis 89*, 647–653.
15. Isetti, G., and Maurer, M. C. (2004) Probing thrombin's ability to accommodate a V34F substitution within the factor XIII activation peptide segment (28−41). *J. Pept. Res. 63*, 241–252.
16. Maurer, M. C., Peng, J. L., An, S. S., Trosset, J. Y., Henschen-Edman, A., and Scheraga, H. A. (1998) Structural examination of the influence of phosphorylation on the binding of fibrinopeptide A to bovine thrombin. *Biochemistry 37*, 5888–5902.
17. Blombaeck, B., Blombaeck, M., Edman, P., and Hessel, B. (1962) Amino-acid sequence and the occurrence of phosphorus in human fibrinopeptides. *Nature 193*, 833–834.
18. Seydewitz, H. H., Kaiser, C., Rothweiler, H., and Witt, I. (1984) The location of a second in vivo phosphorylation site in the A α-chain of human fibrinogen. *Thromb. Res. 33*, 487–498.
19. Martin, S. C., Ekman, P., Forsberg, P. O., and Ersmark, H. (1992) Increased phosphate content of fibrinogen in vivo correlates with alteration in fibrinogen behaviour. *Thromb. Res. 68*, 467–473.
20. Seydewitz, H. H., and Witt, I. (1985) Increased phosphorylation of human fibrinopeptide A under acute phase conditions. *Thromb. Res. 40*, 29–39.
21. Witt, I., and Muller, H. (1970) Phosphorus and hexose content of human foetal fibrinogen. *Biochim. Biophys. Acta 221*, 402–404.
22. Gordon, I. O., and Freedman, R. S. (2006) Defective antitumor function of monocyte-derived macrophages from epithelial ovarian cancer patients. *Clin. Cancer Res. 12*, 1515–1524.
23. Wang, X., Wang, E., Kavanagh, J. J., and Freedman, R. S. (2005) Ovarian cancer, the coagulation pathway, and inflammation. *J. Transl. Med. 3*, 25.
24. Haglund, A. C., Ronquist, G., Frithz, G., and Ek, P. (2000) Alteration of the fibrinogen molecule and its phosphorylation state in myocardial infarction patients undergoing thrombolytic treatment. *Thromb. Res. 98*, 147–156.
25. Ogata, Y., Heppelmann, C. J., Charlesworth, M. C., Madden, B. J., Miller, M. N., Kalli, K. R., Cilby, W. A., Robert Bergen, H., III., Saggese, D. A., and Muddiman, D. C. (2006) Elevated levels of phosphorylated fibrinogen α-isoforms and differential expression of other post-translationally modified proteins in the plasma of ovarian cancer patients. *J. Proteome Res. 5*, 3318–3325.
26. Blomback, B., Blomback, M., Edman, P., and Hessel, B. (1966) Human fibrinopeptides. Isolation, characterization and structure. *Biochim. Biophys. Acta 115*, 371–396.
27. Blomback, B., Blomback, M., and Searle, J. (1963) On the occurrence of phosphorus in fibrinogen. *Biochim. Biophys. Acta 74*, 148–151.
28. Binnie, C. G., Hettasch, J. M., Strickland, E., and Lord, S. T. (1993) Characterization of purified recombinant fibrinogen: Partial phosphorylation of fibrinopeptide A. *Biochemistry 32*, 107–113.
29. Hanna, L. S., Scheraga, H. A., Francis, C. W., and Marder, V. J. (1984) Comparison of structures of various human fibrinogens and a derivative thereof by a study of the kinetics of release of fibrinopeptides. *Biochemistry 23*, 4681–4687.
30. Ni, F., Konishi, Y., Frazier, R. B., Scheraga, H. A., and Lord, S. T. (1989) High-resolution NMR studies of fibrinogen-like peptides in solution: Interaction of thrombin with residues 1−23 of the A α-chain of human fibrinogen. *Biochemistry 28*, 3082–3094.
31. Scheraga, H. A. (1983) Interaction of thrombin and fibrinogen and the polymerization of fibrin monomer. *Ann. N.Y. Acad. Sci. 408*, 330–343.
32. Scheraga, H. A. (1986) Chemical basis of thrombin interactions with fibrinogen. *Ann. N.Y. Acad. Sci. 485*, 124–133.
33. Martin, P. D., Robertson, W., Turk, D., Huber, R., Bode, W., and Edwards, B. F. (1992) The structure of residues 7−16 of the A α-chain of human fibrinogen bound to bovine thrombin at 2.3-Å resolution. *J. Biol. Chem. 267*, 7911–7920.
34. Bode, W., Turk, D., and Karshikov, A. (1992) The refined 1.9-Å X-ray crystal structure of D-Phe-Pro-Arg chloromethylketone-inhibited human α-thrombin: Structure analysis, overall structure, electrostatic properties, detailed active-site geometry, and structure-function relationships. *Protein Sci. 1*, 426–471.
35. Ni, F., Meinwald, Y. C., Vasquez, M., and Scheraga, H. A. (1989) High-resolution NMR studies of fibrinogen-like peptides in solution: Structure of a thrombin-bound peptide corresponding to residues 7−16 of the A α-chain of human fibrinogen. *Biochemistry 28*, 3094–3105.
36. Ni, F., Zhu, Y., and Scheraga, H. A. (1995) Thrombin-bound structures of designed analogs of human fibrinopeptide A determined by quantitative transferred NOE spectroscopy: A new structural basis for thrombin specificity. *J. Mol. Biol. 252*, 656–671.
37. Ni, F., Ripoll, D. R., Martin, P. D., and Edwards, B. F. (1992) Solution structure of a platelet receptor peptide bound to bovine α-thrombin. *Biochemistry 31*, 11551–11557.
38. Mathews, I. I., Padmanabhan, K. P., Ganesh, V., Tulinsky, A., Ishii, M., Chen, J., Turck, C. W., Coughlin, S. R., and Fenton, J. W., II. (1994) Crystallographic structures of thrombin complexed with thrombin receptor peptides: Existence of expected and novel binding modes. *Biochemistry 33*, 3266–3279.
39. Stubbs, M. T., Oschkinat, H., Mayr, I., Huber, R., Angliker, H., Stone, S. R., and Bode, W. (1992) The interaction of thrombin with fibrinogen. A structural basis for its specificity. *Eur. J. Biochem. 206*, 187–195.
40. Sabo, T. M., Farrell, D. H., and Maurer, M. C. (2006) Conformational analysis of γ′ peptide (410−427) interactions with thrombin anion binding exosite II. *Biochemistry 45*, 7434–7445.
41. Isetti, G., and Maurer, M. C. (2004) Thrombin activity is unaltered by N-terminal truncation of factor XIII activation peptides. *Biochemistry 43*, 4150–4159.
42. Bah, A., Chen, Z., Bush-Pelc, L. A., Mathews, F. S., and Di Cera, E. (2007) Crystal structures of murine thrombin in complex with the extracellular fragments of murine protease-activated receptors PAR3 and PAR4. *Proc. Natl. Acad. Sci. U.S.A. 104*, 11603–11608.
43. Lee, I. H., Chung, S. I., and Lee, S. Y. (2002) Effects of Val34Leu and Val35Leu polymorphism on the enzyme activity of the coagulation factor XIII-A. *Exp. Mol. Med. 34*, 385–390.
44. Andersen, M. D., Kjalke, M., Bang, S., Lautrup-Larsen, I., Becker, P., Andersen, A. S., Olsen, O. H., and Stennicke, H. R. (2009) Coagulation factor XIII variants with altered thrombin activation rates. *Biol. Chem. 390*, 1279–1283.
45. Sadasivan, C., and Yee, V. C. (2000) Interaction of the factor XIII activation peptide with α-thrombin. Crystal structure of its enzyme-substrate analog complex. *J. Biol. Chem. 275*, 36942–36948.
46. Nair, D. G., Sunilkumar, P. N., and Sadasivan, C. (2008) Modeling of factor XIII activation peptide (28−41) V34L mutant bound to thrombin. *J. Biomol. Struct. Dyn. 26*, 387–394.
47. Yee, V. C., Pedersen, L. C., Bishop, P. D., Stenkamp, R. E., and Teller, D. C. (1995) Structural evidence that the activation peptide is not released upon thrombin cleavage of factor XIII. *Thromb. Res. 78*, 389–397.